Wear Testing of a Canine Hip Resurfacing Implant That Uses Highly Cross-linked Polyethylene

Kevin J. Warburton,[1] John B. Everingham,[1] Jillian L. Helms,[1] Andrew J. Kazanovicz,[2] Katherine A. Hollar,[1] Jeff D. Brourman,[3] Steven M. Fox,[2] Trevor J. Lujan[1]

[1]Boise State University, 1910 University Drive, Boise 83725-2085, Idaho, [2]Securos Surgical, 443 Main Street, Fiskdale 01518, Massachusetts, [3]WestVet Animal Emergency and Specialty Center, 5019 N. Sawyer Ave., Garden City 83714, Idaho

Received 27 March 2017; accepted 13 September 2017
Published online in Wiley Online Library (wileyonlinelibrary.com). DOI 10.1002/jor.23745

ABSTRACT: Hip resurfacing offers advantages for young, active patients afflicted with hip osteoarthritis and may also be a beneficial treatment for adult canines. Conventional hip resurfacing uses metal-on-metal bearings to preserve bone stock, but it may be feasible to use metal-on-polyethylene bearings to reduce metal wear debris while still preserving bone. This study characterized the short-term wear behavior of a novel hip resurfacing implant for canines that uses a 1.5 mm thick liner of highly cross-linked polyethylene in the acetabular component. This implant was tested in an orbital bearing machine that simulated canine gait for 1.1 million cycles. Wear of the liner was evaluated using gravimetric analysis and by measuring wear depth with an optical scanner. The liners had a steady-state mass wear rate of 0.99 ± 0.17 mg per million cycles and an average wear depth in the central liner region of 0.028 mm. No liners, shells, or femoral heads had any catastrophic failure due to yielding or fracture. These results suggest that the thin liners will not prematurely crack after implantation in canines. This is the first hip resurfacing device developed for canines, and this study is the first to characterize the in vitro wear of highly cross-linked polyethylene liners in a hip resurfacing implant. The canine implant developed in this study may be an attractive treatment option for canines afflicted with hip osteoarthritis, and since canines are the preferred animal model for human hip replacement, this implant can support the development of metal-on-polyethylene hip resurfacing technology for human patients. © 2017 Orthopaedic Research Society. Published by Wiley Periodicals, Inc. J Orthop Res

Keywords: cross-linked polyethylene; hip simulator; gravimetrics; dog; surface wear

Hip osteoarthritis is a debilitating and irreversible disease that damages the articular cartilage in the hip joint. In the United States, the lifetime risk of symptomatic hip osteoarthritis is approximately 25% for humans,[1] while 20% of adult canines and 80% of geriatric canines suffer from osteoarthritis,[2] with the highest incidence of canine osteoarthritis occurring in the hip.[3] The standard treatment for humans and canines with hip osteoarthritis is a total hip arthroplasy (THA). In THA, the damaged femoral head is surgically removed and the femoral shaft and acetabulum are reamed to prepare for replacement with a prosthetic femoral and acetabular component. Traditionally, the THA femoral component consists of a metallic femoral head (ball) and stem, and the acetabular component consists of a metallic shell and polymeric cup made of ultrahigh-molecular-weight polyethylene. Although THA has been highly successful at relieving pain and returning elderly patients to moderate activity levels, THA is less ideal for younger human patients. For example, implant survival in younger patients does not reach 10 years in 28% of cases.[4] Although THA revision surgeries are feasible, they have less favorable outcomes than primary THA and can result in decreased joint stability.[5,6]

Another option for human patients with hip osteoarthritis is hip resurfacing, where surgeons "resurface" the hip joint by fitting it with a thin acetabular cup and femoral head. Hip resurfacing, introduced in 2006, better mimics the natural hip anatomy, and compared to THA, it has several major benefits that include: bone preservation that facilitates future conversion to conventional stemmed prosthesis,[7,8] low dislocation risk due to the large femoral head diameter, physiological hip loading that prevents stress shielding, more natural gait, and a return to more high-impact sporting activities.[5,6,9,10] Despite these advantages, hip resurfacing has not been widely adopted, due partly to complications related to metal wear debris generated by the metal-on-metal (MoM) bearing surfaces, such as metallosis and pseudotumors.[11–15] A reason MoM bearings are traditionally used in hip resurfacing is because the limited amount of bone stock around the acetabulum places inherent size constraints on the thickness of the acetabular component. This geometric constraint has precluded the use of conventional polyethylene liners in hip resurfacing devices. For example, commercial MoM hip resurfacing implants have acetabular components with a total thickness of 3 mm, while a recommended minimal thickness for a metal-on-polymer (MoP) bearing surface using a conventional polyethylene liner, not including the metal backing, is 6 mm.[16] One option to reduce the liner thickness is to replace the conventional polyethylene with highly cross-linked polyethylene, which is a more wear resistant and durable material.[17] In recent

Conflicts of interest: Conflicts of interest include being a paid employee for Securos Surgical (AJK, SF), receiving royalties, and consulting fees from MWI (JDB), consulting for r-NAV and Aratana (SF), and owning stock in MWI (SF).
Grant sponsor: National Institute of General Medical Sciences; Grant number: P20GM109095; Grant sponsor: Idaho Global Entrepreneurial Mission.
Correspondence to: Trevor J. Lujan (T: +1-208-426-2857; F: +1-208-392-1589; E-mail: trevorlujan@boisestate.edu)

prospective studies by Pritchett[16] and Amstutz et al.,[18] hip resurfacing implants that used a highly cross-linked polyethylene liner had a 97% and 81% Kaplan–Meier survivorship at 10 years, respectively. Although results from these studies are encouraging, the acetabular component used in these studies was still over twice as thick as a standard MoM hip resurfacing device. In addition, in vitro wear testing was not conducted on these implants, and a wear analysis was only available from a limited number of retrieved specimens. Nevertheless, highly cross-linked polyethylene has potential to bring a renewed interest in using MoP hip resurfacing for younger patients.[19]

The potential clinical adoption of MoP hip resurfacing implants could be expedited with an appropriate animal model to test this technology. The canine is the animal model of choice for THA,[20,21] where the performance of canine hip implants is most comparable to young, active human patients.[22,23] Federal regulation of veterinary medical devices is less stringent than human medical devices, and therefore developing a canine hip resurfacing implant that uses highly cross-linked polyethylene could permit more rapid assessment of in vivo device performance.

The objective of this research was to characterize the wear of a novel hip resurfacing implant for canines that uses a highly cross-linked polyethylene liner. The acetabular component of this implant is the first to have a thickness equivalent to MoM hip resurfacing implants. This experimental study will determine if the thin liners will fracture or experience excessive wear during over a million cycles of in vitro testing.

METHODS

A new hip resurfacing device for canines was developed that incorporates a thin cross-linked polyethylene liner in the acetabular component. This device was tested for wear behavior in a canine hip simulator for 1.1 million cycles. Wear of the polymer liner was evaluated using gravimetric analysis, light microscopy, and 3D optical scanning.

Hip Resurfacing Implant

Prototype hip resurfacing implants were developed that consist of three parts: An acetabular shell, an acetabular liner, and a femoral head (Fig. 1; Securos Surgical, Fiskdale, MA). The acetabular shells were made of titanium (Ti–6AL–4V) and were machined to a uniform thickness of 1 mm. The acetabular liners were manufactured using highly cross-linked polyethylene powder (GUR 1020; Celanese, Irving TX), and were compression molded into their stock form between 190–200°C (PPD Meditech, Quebec Canada). Cross-linking was achieved using 75 kGy of gamma irradiation, and the annealing process used a ramp up to 105°C and a slow cool of 5–10°C per hour. A 5-axis milling machine was used to dry machine the acetabular cup to have an inner diameter of 24 mm and a uniform thickness of 1.5 mm. Terminal sterilization was performed using ethylene oxide per ISO 11135 (Sterigenics, Oakbrook IL).[24] Tabs were included on the outer circumference of the liner to prevent rotation when press-fit into the metallic shell. The femoral heads were cobalt chromium with a diameter of 24 mm and were coated with titanium niobium nitride (Ti–Nb–N). The surface roughness of the femoral head was ~0.77 microns.

Canine Hip Simulator

Wear testing was performed using a custom hip simulator (Fig. 2A). The simulator is a single-axis orbital bearing machine (OBM) that was built according to international standards for wear testing of human hips[25]; however, it was modified to reproduce hip kinematics of an adult medium-sized canine. The hip simulator consists of two chambers filled with lubricant, each housing one implant. The top chamber houses a "load soak control" implant that is only subjected to axial loading while the bottom chamber houses a "wear" implant that is subjected to axial and torsional loading. The titanium shells and femoral heads in both chambers were centered and fastened into separate holding fixtures (Fig. 2B and C). Dental cement was used to fasten the implants (Fricke International Inc., Streamwood, IL; Vitacrilic), and required the adhered surfaces of the metal shell to be roughened with 120 grit sandpaper. The holding fixture (Fig. 2B) for the wear implant was connected to a pin and block single universal joint to self-align the femoral cup and head during the simulated gait cycle.

The hip simulator was bolted onto an electrodynamic mechanical test system (Instron, Norwood, MA; E10000), and a vertical axial load was applied to the load soak control implant (Fig. 2A). This axial load was applied in force control at 2 Hz from 10 to 211 N (Instron, Norwood, MA; 1kN Dynacell 2527, error = 0.4%), and was directly transferred to the wear implant through a spring fixture. The wear implant

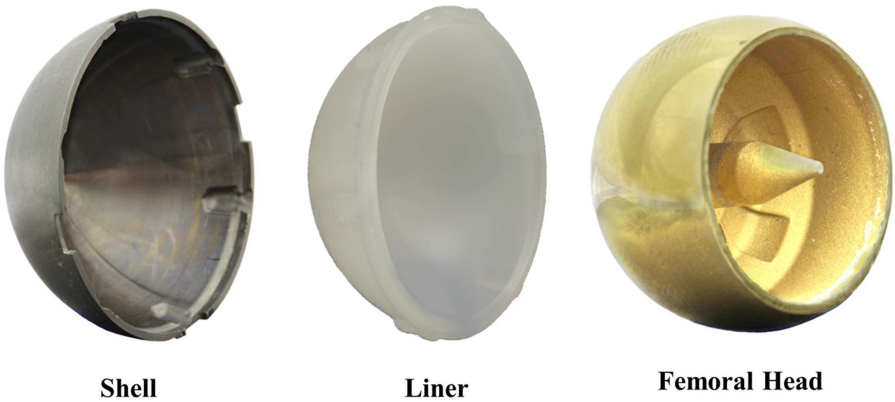

Figure 1. Components of the canine hip resurfacing implant.

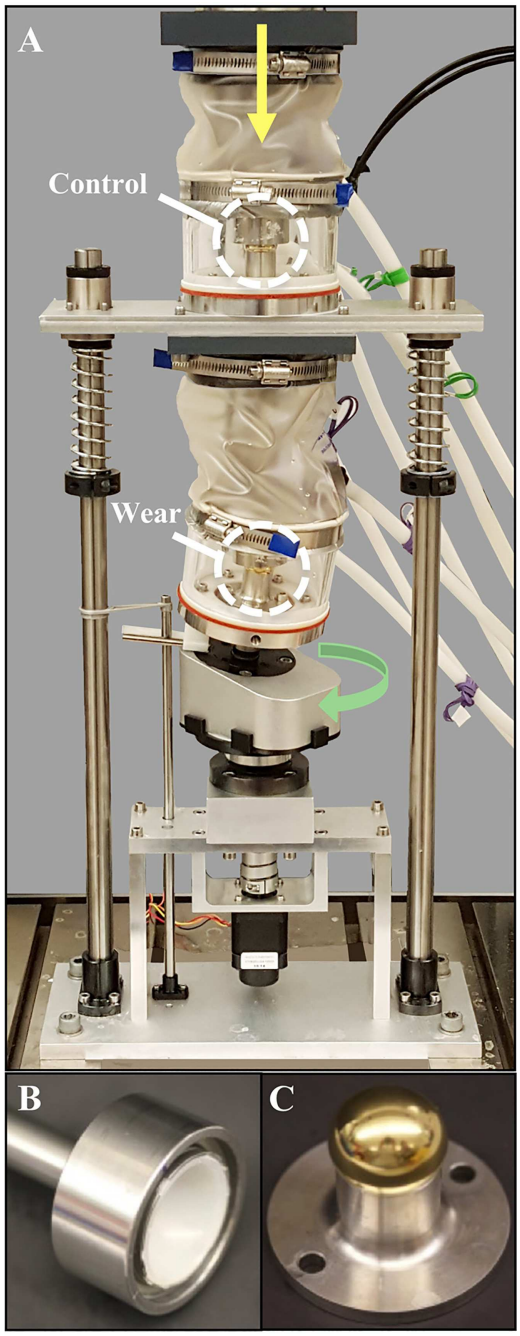

Figure 2. Canine hip simulator. (A) An axial load (yellow arrow) is applied to both the load soak control and wear implants, but only the wear implant is rotated (green arrow). (B) The titanium shell and (C) CoCr femoral head were cemented into hip simulator fixtures.

was simultaneously rotated using a high torque rotary motor (Anaheim Automation, Anaheim, CA; NEMA 17). To synchronize the linear and rotational motion, waveform signals were concurrently sent to the motors using a custom LabVIEW program (National Instruments, Austin, TX). The waveform signal for the linear load was sent to the mechanical test system console, which applied the loading profile in force control using a feedback loop. The testing system was programmed to apply a peak load of 211 N during the stance phase (0–45% of the gait cycle) and a minimum load of 10 N during the swing phase (45–100% of the gait cycle). The magnitude and timing of this loading profile was based on published experimental measurements of an adult medium-sized canine at a trot.[26] The measured axial load and rotary position were recorded by the LabVIEW software to verify that the load was being properly applied during the gait cycle (Fig. 3A). There was a very strong positive correlation between the targeted and measured load during stance phase ($R^2 = 0.94$).

The OBM design enables three axes of motion to occur between the bearing surfaces of the wear implant. These axes of motion correspond to the clinical rotations of flexion-extension (FE), abduction-adduction (AA), and internal-external rotation (IER). The slope of the slanted base component controls the amplitude of FE and AA, while the vertical position of the rotation-prevention lever controls the amplitude of IER.[27] These OBM design parameters were selected to produce values for FE, IER, and AA that best matched the kinematics that have been experimentally measured for an adult medium-sized canine (Fig. 3B–D).[28]

Kinematic Validation of the Hip Simulator

A test procedure was developed to validate that our OBM hip simulator design did successfully reproduce the hip kinematics of an adult canine, where the clinical rotations of the hip simulator were quantified using Euler angles and a structured-light 3D scanner (LMI Technologies, Delta, Canada). For this analysis, the "static" acetabular cup and "rotating" femoral head in the bottom chamber of the hip simulator were replaced by coordinate system triads (Fig. 4A and B). When attached to the hip simulator, the origin of these coordinate system triads corresponded to the centroids of the cup and head. These triads were imaged with the 3D scanner at 90° increments, which corresponded to where the local maximum, local minimum, and inflection points of the FE, IER, and AA rotations would exist. Three-dimensional reconstructions of the static and rotating triads were generated at each angle increment (Flexscan; LMI Technologies, Delta, Canada). Orthonormal coordinate systems were formulated by taking cross products of vectors measured from the point cloud data of the triad axes.[29] The transformation matrix between the stationary and rotating coordinate systems was calculated at each angle increment, and a back calculation of the Euler angle values for FE, IER, and AA was computed using established methods.[30] Since the physical constraints of the OBM will prescribe sinusoidal curves for all three rotation waveforms, a three-parameter sine function was fit to these experimental data points using a non-linear least squares fitting approach (Fig. 3B–D). This analysis determined that the OBM hip simulator could reasonably reproduce the FE and IER kinematics of a canine ($R^2 = 0.78$ and 0.61, respectively; Fig. 3D), but the simulator could not reproduce the AA kinematics ($R^2 = 0.21$; Fig. 3D).

To visualize the differences between the kinematics produced by the hip simulator and an adult canine, slide tracks were calculated on a unit sphere. For this analysis, the FE, IER, and AA waveforms for the hip simulator and adult canine in Fig. 3B–D were merged into time-dependent transformation matrices. Using an established methodology, these transformation matrices were used to determine the slide tracks of three fixed points on the polymer liner that were articulating against the femoral head during one gait cycle (Fig. 4C). Slide tracks from the hip simulator were qualitatively similar to the slide tracks measured in an adult

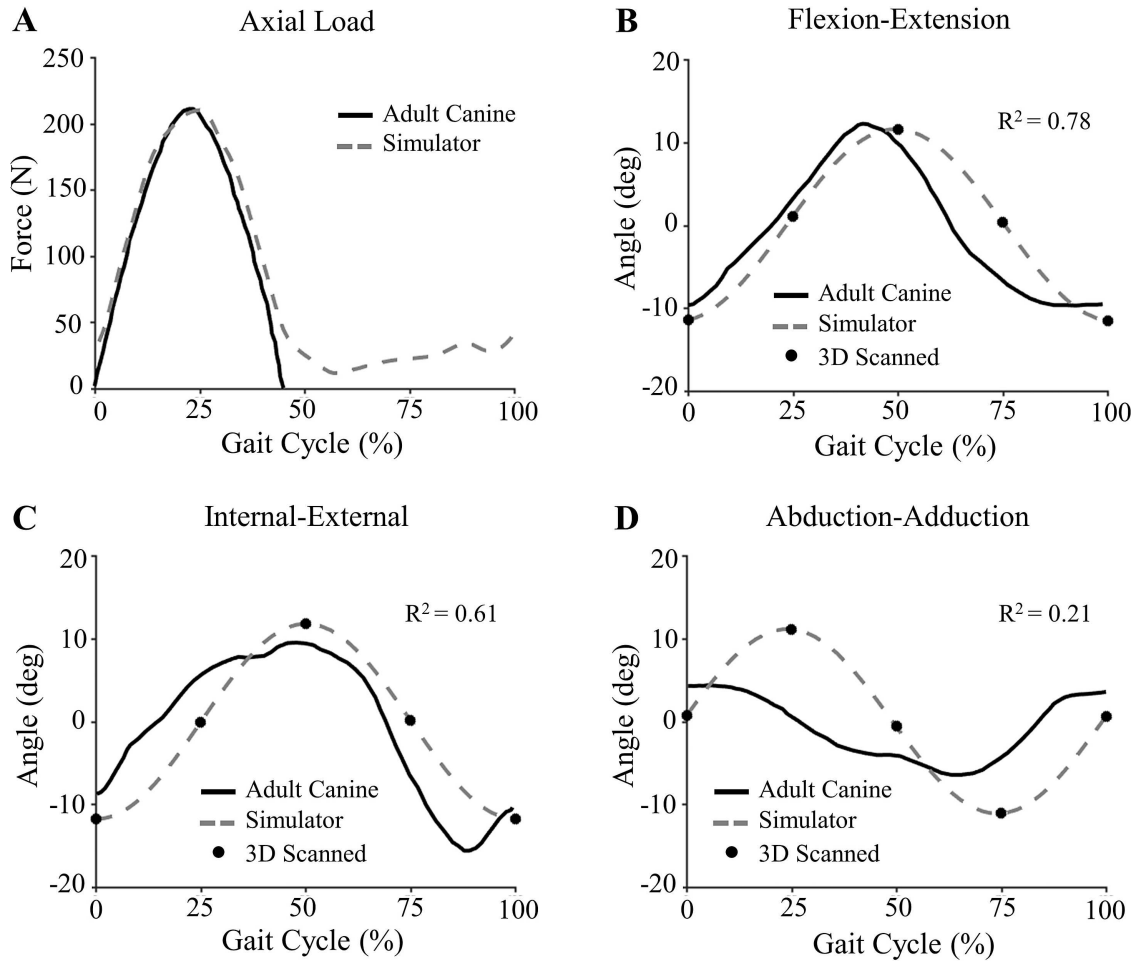

Figure 3. Hip simulator kinetics and kinematics. (A) Loading profiles of the hip simulator and an adult canine during gait. (B–D) Clinical rotations of the hip simulator and an adult canine during gait. The simulator waveform (dashed) was fit to data points that were experimentally measured using a 3D optical scanner, and was compared to kinematic data from an adult canine (solid). Note: The 0% and 100% gait cycle use the same scanned data.

canine, and this qualitative comparison was comparable to hip simulators used for human hip prostheses.[31]

Wear Testing

The hip resurfacing implants were each wear tested in the canine hip simulator for 1,100,000 cycles of loading at 2 Hz, broken into four stages of 275,000 cycles (Fig. 5). Wear testing was performed on four load soak control implants and four wear implants. This sample size complied with standards for gravimetric wear assessment of prosthetic hip designs in simulator devices.[32] Prior to wear testing, the implants in each chamber were lubricated with 400 ml of

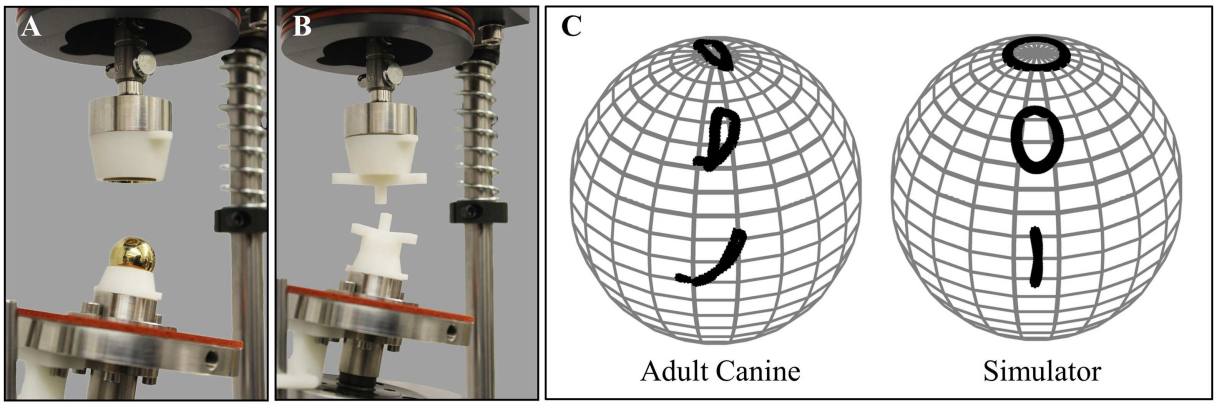

Figure 4. Kinematic validation of canine hip simulator. (A) Hip resurfacing implant in simulator. (B) Replacement of the hip resurfacing implant with triads to create coordinate systems. (C) Slide tracks of three points on the femoral head using left) kinematic data measured from an adult canine and right) kinematic data from the hip simulator.

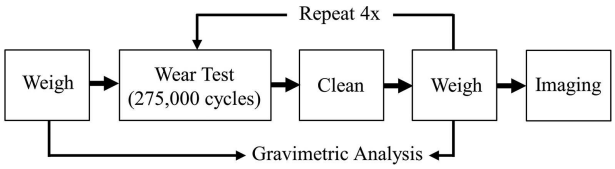

Figure 5. Flow chart for wear testing and analysis.

bovine calf serum that had been diluted with deionized water to a protein concentration of 2.5 g/100 ml (Hyclone Laboratories, Logan, UT). During wear testing, it was necessary to add additional deionized water to replenish fluid lost from evaporation or small leaks in the O-rings, but in keeping with international standards, the serum was never diluted below a protein concentration of 2.0 g/100 ml.[25] The bovine serum was heated in external tanks and circulated through each chamber using a peristaltic pump to prevent contamination of the serum. Temperature sensors in each chamber and external heating plates were used to monitor and maintain the temperature in each chamber to a targeted canine body temperature of 38°C. The bovine serum in each chamber was fully changed every 550,000 cycles.

The peak axial load and chamber temperatures were recorded every 550 cycles to verify the consistency of test conditions during the 1.1 million cycle experiment (Table 1). Results for each test showed that temperature and peak loads were on average kept within 3% and 1% of targeted values, respectively. The rotary motor position was sampled at the beginning, middle, and end of each testing stage to verify that the linear and rotational motion were properly synchronized (Fig. 3A).

Gravimetric wear analysis was performed every 275,000 cycles (Fig. 5).[33] Prior to wear testing, liners were initially weighed after presoaking in diluted bovine serum for 48 hours. After each 275,000 cycle testing stage, implants were removed from their test chamber, cleaned, and dried using established protocols.[33] The weight of the load soak control liner, w_i^{ctrl}, and wear liner, w_i^{wear}, at each testing stage, i, were acquired by taking the average of 3 weight measurements using a microbalance (AT201; Mettler-Toledo AG, Greifensee, Switzerland; readability = 0.01 mg, sensitivity = 0.00015%, reproducibility = 0.015 mg). If two successive measurements of the same specimen were not within 0.1 mg, the measurements were repeated until the successive measurements were within 0.1 mg.[33] The net mass loss of the liner, W_i, was then calculated at each testing stage by adding the weight gain of the load soak control liners between testing stages to the weight loss of the wear liners between the testing stages (Equation 1).[33] Note that w_0^{wear} and w_0^{ctrl} represent the initial weight measurement of the wear and control implants respectively before testing, and consider that $W_0 = 0$ for this notation.

$$W_i = \left(\Sigma_0^{i-1} W_i\right) + \left(w_{i-1}^{\text{wear}} - w_i^{\text{wear}}\right) + \left(w_i^{\text{ctrl}} - w_{i-1}^{\text{ctrl}}\right), i = \{1,2,3,4\} \quad (1)$$

Using W_i from Equation (1), a least squares linear regression was used to fit parameters in Equation (2).[33] Here, a_G is the mass wear rate, n represents the number of cycles, and b is a constant.

$$W_i = a_G \times n + b, i = \{1,2,3,4\} \quad (2)$$

Wear data from the first 275,000 cycles was not considered in the wear rate calculation since the wear rate had not yet reached a steady-state condition.[34] The associated volumetric wear rate, $a_{G\text{volume}}$, was computed using the density of the liner ($\rho = 0.932$ g\cm^3).

Table 1. Temp and Load Measured During 1.1 Million Cycle Tests

	Temperature (°C)		Axial Load
Test #	Control	Wear	(*N*)
1	36.8 ± 0.6	38.2 ± 0.4	208.8 ± 0.9
2	37.1 ± 1.0	38.1 ± 0.3	209.3 ± 0.7
3	36.7 ± 1.5	37.8 ± 0.7	209.1 ± 0.8
4	37.4 ± 1.5	38.5 ± 0.4	209.2 ± 0.8
All	37.0 ± 1.2	38.2 ± 0.5	209.1 ± 0.8

Image Analysis

After wear testing and gravimetric analysis were completed, the polymer liners were imaged to analyze surface wear topology. To detect scratch patterns on each implant surface, digital images were taken using a stereo microscope at 20× magnification (AmScope, Irvine, CA). The wear depth was then measured using the previously mentioned structured-light 3D optical scanning system. In preparation for scanning, each load soak control and wear liner were finely airbrushed from 10 to 12 inches away with 1/4 teaspoon of hexagonal boron nitride dissolved in 6 ml of acetone. Individual liners were securely press fit into a titanium shell cemented into a custom stand. Each individual liner and stand was scanned 11 times in increments of 10° over a total range of 100°. These scans were then combined into individual 3D models consisting of on average 1.84 million points per liner. To measure the wear depth, the 3D models of the wear liner and matching load soak control liner were aligned based on the stand geometry, and the difference between these models was due to wear. The accuracy of this 3D scanning procedure was quantified using a delrin reference block with known wear depths; and this validation procedure determined that the 3D scanner can measure 10 μm of wear with 16% error and 20 μm of wear with 8% error.

Statistical Analysis

An ANOVA test was performed to determine the effect of test cycles on the net mass loss. The linearity of steady-state wear was determined using the coefficient of determination (R^2). For all statistical tests, significance was set to a $p < 0.05$.

RESULTS

Steady-state wear was achieved after 275,000 cycles (Fig. 6; $R^2 = 0.99$). The liners had an average steady-state mass wear rate of 0.99 mg per million of cycles (Mc) and an average steady-state volumetric wear rate of 1.06 mm^3/Mc (Table 2). The wear rate during the first stage of 275,000 cycles was 3.9 mg/Mc, which was significantly greater than the other three stages

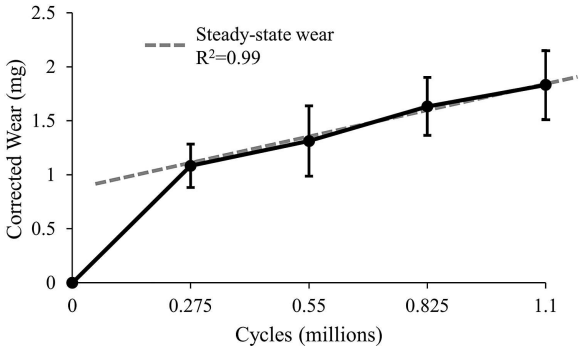

Figure 6. Wear behavior of the acetabular liners. Steady-state wear (dashed line) was reached after 275,000 cycles. Error bars = standard deviation.

(Fig. 6; $p < 0.001$). After 1.1 million cycles, the weight gain in the four load soak control liners was 0.04 ± 0.20 mg.

No liners, shells, or femoral heads had any catastrophic failure due to cracking or fracture. Visual examination by stereomicroscopy revealed scratching on the articular surface of all liners subjected to wear testing (Fig. 7). The average wear depth for the four liners was 19.6 ± 7 μm. The average wear depth in the central regions of the four liners was 28.0 ± 10 μm (Fig. 8), where the central region was defined to have approximately 15% of the liner's total surface area. Cup distortion was evident, as the liner material had asymmetric wear patterns in three of the four wear tested implants, with localized regions of elevated and depressed surfaces (Fig. 8).

DISCUSSION

The enhanced wear resistance of cross-linked polyethylene has expanded design options for hip replacement devices. The goal of this study was to incorporate a thin liner of radiated cross-linked polyethylene into a hip resurfacing device for canines. To our knowledge, this is the thinnest polyethylene liner yet developed for a hip resurfacing or THA device. The polymer liner did not fracture and showed acceptable wear after 1.1 million cycles of in vitro testing. Results from this study will be useful to veterinary surgeons interested in implanting this device into canines.

The incorporation of polyethylene liners into hip resurfacing implants is a relatively new design strategy. While an advantage of this strategy is the elimination of metal wear debris, a clear challenge has been designing a thin two-piece acetabular component that preserves the acetabular bone stock. Initial designs of polyethylene hip resurfacing used conventional polyethylene, which resulted in high rates of aseptic loosening and osteolysis.[35–37] A more recent prospective study by Pritchett examined 190 hip resurfacing procedures that used a two-piece acetabulum component that included a 3.8 mm thick highly cross-linked polyethylene liner.[16] This 3.8 mm liner had previously been used successfully in THA,[38] and the Pritchett study was similarly successful with a Kaplan–Meier survivorship of 97%. Pritchett stated that two notable concerns of fabricating cross-linked polyethylene liners that are thinner than 3.8 mm is that the liners would be prone to fracture and the metal shell and liner would be susceptible to abnormal cup deformation.[39]

Veterinary medicine presents a pragmatic environment to test the efficacy of using highly cross-linked polyethylene liners that are thinner than 3.8 mm for several reasons. First, canines are highly active, and canine hip implants are considered a reasonable model for human hip implants that target younger human patients with an active lifestyle.[22,23] Second, veterinary medical devices do not require pre-market approval from the U.S. Food and Drug Administration, and therefore the iterative product development process between in vivo results and design modifications can be expedited. Third, hip osteoarthritis is highly prevalent in many canine breeds,[1] and hip resurfacing may be an attractive treatment option as the larger diameter femoral head can support the strenuous activity levels that canines want to naturally return to post-surgery. Therefore, not only can canine hip resurfacing serve as a valuable animal model to evaluate and optimize the design of MoP hip resurfacing implants for humans, but hip resurfacing has potential to be an advantageous treatment of hip osteoarthritis for canines.

The present study has developed a new canine hip resurfacing implant with a two-piece acetabular component that has a cross-linked polyethylene liner with a wall thickness of 1.5 mm. This liner thickness was selected to maximize bone preservation in the canine acetabulum while also maintaining structural integrity. For a locking mechanism, tabs on the polyethylene liner were press fit into grooves along the inner circumference of the titanium shell. To cross-link the polyethylene, a high irradiation dose of 75 kGy was selected to increase wear resistance and shelf life. The aggregate thickness of the polyethylene liner and the metal shell is 2.5 mm, which is less than the thickness of MoM hip resurfacing implants for humans. For this in vitro experiment, the metal shell had a smooth backing, but for future clinical applications this would need to be modified to have a porous backing for cementless implantation.

Table 2. Gravimetric Wear Results

Test #	Mass Wear Rate[a] (mg/10^6 Cycles)	Volumetric Wear Rate[a] (mm^3/10^6 Cycles)
1	1.06	1.14
2	1.20	1.29
3	0.89	0.95
4	0.81	0.87
All	0.99 ± 0.17	1.06 ± 0.19

[a]Steady-state wear rate with load soak control correction.

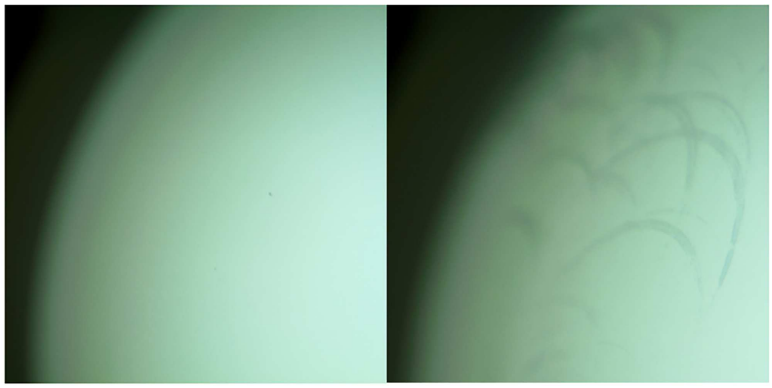

Figure 7. Stereomicroscopy of liner surface for a left) control specimen and right) wear specimen. Scratching is evident in the wear specimen.

The hip simulator developed in this study has enabled for the first time the assessment of wear behavior in a hip replacement prosthesis for canines (THA or hip resurfacing). Furthermore, to the authors' knowledge, this is the first in vitro wear assessment of a hip resurfacing implant that uses a highly cross-linked polyethylene liner (human or canine). The in vitro measurement of wear behavior from joint simulators is a cost-effective method to detect design flaws in implant designs prior to clinical trials.[40] The design of our OBM hip simulator was based on international standards for human hip simulators with modifications to simulate the kinematics of canine gait. Although the FE and IER waveforms produced by our hip simulator were a good match with in-vivo canine kinematics ($R^2 = 0.78$ and 0.62, respectively), the AA waveform was a poor match ($R^2 = 0.21$). This is an inherent limitation of the OBM design, but it's important to note that the overall wear characteristics of hip implants are still well predicted using OBMs.[25,27]

The wear rate of each thin liner was estimated by simulating 1.1 million gait cycles with the OBM. In the first 275,000 cycles, we observed a high initial wear rate of 3.9 mg/Mc (Fig. 6), which is consistent with running-in or run-in wear that has been observed and discussed in human hip simulator studies.[41–44] The physical reason for high run-in wear is that the contacting surfaces of the femoral head and polyethylene liner are conforming to each other as non-ideal surface irregularities are worn away.[44] After 275,000 cycles, the wear rate became steady-state at 0.99 mg/Mc (Fig. 6). The linearity of our steady-state region ($R^2 = 0.99$) was comparable to the steady-state linearity measured in previous human hip simulator studies (R^2 range = 0.90–1.00).[43,45] These results indicate that the 1.1 million duration of this short-term study was able to estimate the run-in wear and steady-state wear of the canine MoP bearing. Although test durations of five million cycles are recommended to fully characterize bearings in human hip implants,[25] simulator studies have also used short-term tests between 0.5 and 2.5 million cycles to evaluate wear in human THA,[45–48] which is reasonable since the wear of cross-linked polyethylene in simulators is consistently shown to be highly linear with cycle count and hence predictable once a steady-state wear rate is achieved.[42,43,49–51] Therefore, the steady-state wear rate of 0.99 mg/Mc measured in this short-term study is likely a reliable estimate for the canine hip implant.

The wear rates measured in this canine study can be compared to previous human research that uses gamma cross-linked polyethylene. Our steady-state wear rate of 0.99 mg/Mc is 2.4× less than a study by Saikko et al.[52] that examined gamma cross-linked polyethylene in human THA (irradiation dose = 95 kGy). We would have expected a greater difference in wear rates, since canine implants experience approximately 10× less load than human implant wear tests, and a previous study of postmortem-retrieved canine hip implants found the volumetric wear rates of conventional polyethylene liners are 10× greater in humans than in canines.[22,23] A potential explanation for the relatively high wear results in our study is that the surface roughness of our femoral head components

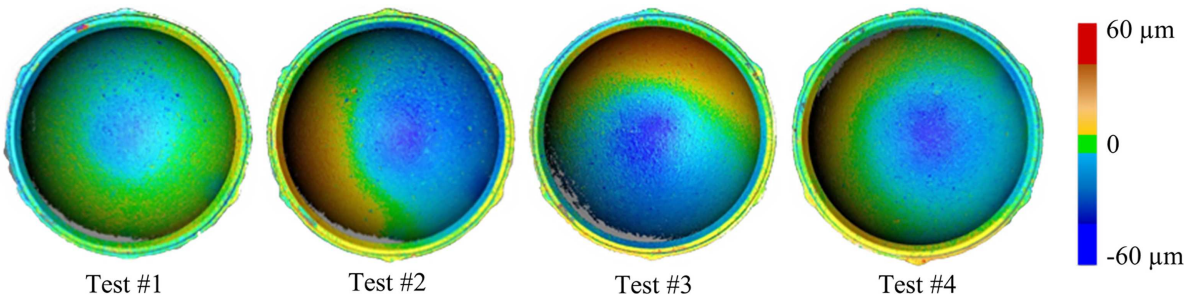

Figure 8. Three-dimensional colorimetric maps showing wear depth of liners after 1.1 million cycles.

($R_a = 0.77\,\mu m$; Fig. 1) was fifteen times greater than the standard roughness of femoral heads used in human studies ($R_a = 0.05\,\mu m$). This explanation seems justified, since wear and morphological changes in highly cross-linked polyethylene liners have been shown to rapidly increase with small rises in femoral head surface roughness.[50,53] The reason a high surface roughness was selected for our study was to provide a "worst-case" scenario to rigorously test whether the thin cross-linked polyethylene liners would experience excessive wear or fracture during testing. It is important to note that any comparison between the wear behavior of human and canine THA should be treated with caution, as intrinsic differences exist in joint kinematics, loading magnitudes, and implant sizing. Nonetheless, the canine is the animal model of choice for THA,[21–23] and since this is the first study to develop a cross-linked polyethylene implant for canines and the first study to develop a hip simulator for canines, there are no previously published in vitro studies of canine hip implants that can be used for comparison.

The surface wear of our cross-linked polyethylene liner was measured using structured-light 3D scanning. While deformation of the acetabular component has historically not been a clinical problem when thick polyethylene liners are used in THA, it does become a concern when the polyethylene liner is very thin.[39] Our imaging analysis revealed that most of the wear was centralized evenly around the vertical loading path of the simulator, and had an average wear depth of 0.028 mm. It is estimated that a healthy canine has 10,000 loading cycles per day,[54] equating to 3.65 million cycles per year. The annual surface wear is therefore estimated to be 6.7% of the 1.5 mm liner thickness per year. Both these estimates are based on average surface wear in the central region of the liner, where surface wear was greatest. It is worth noting that the average estimates of surface wear may underestimate the wear penetration occurring in small, localized regions. Conversely, the number of cycles per day is based on a healthy dog and may overestimate canine activity after hip surgery. Uneven wear of the polyethylene liner was evident, with the liner surface area having elevated regions near the outer ring in Figure 8, which may have been caused by small differences in deformation of the hemispherical cup geometry between the control and wear implants. The colorimetric maps of wear depth in Figure 8 were calculated using reference dimensions from the load soak control per international standards.[33] Therefore the figures should represent material loss and not plastic deformation (creep) associated with "bedding in,"[55] which is accounted for in the load soak control and is expected to occur within the first 500,000 cycles.[33,55,56] Since "bedding in" is a function of cyclic creep, the annual activity level of the patient, whether human or canine, should not affect the number of cycles until "bedding in" is complete. Therefore, even if a canine implant experiences 3.65 million cycles per year, the "bedding in" period would still be expected to occur within the first 500,000 cycles. Finally, circular scratches were noticeable on the polyethylene surface of the wear group, which is common for cross-linked and conventional polyethylene liners tested in hip simulators.[57]

There are several limitations to this study. First, the duration of the wear test in this study was 1.1 million cycles, and would be classified as a short-term test.[46,48] Nevertheless, this duration enabled us to observe run-in wear and steady-state wear, and thereby provides a preliminary wear characterization of this new implant. Second, the specimens in the hip simulator were concentrically mounted, and more accurate wear behavior could be acquired by using an anatomical approach, where the femoral and acetabular components are positioned at a physiological angle relative to each other. This could result in different wear patterns since the wear would be concentrated closer to impingement locations.[25] Yet, the concentric mounting approach used in this study gave reasonable slide tracks (Fig. 4C) and is an established methodology for wear testing.[27] Third, the size of the polyethylene wear debris was not measured in this study, and the size of these particulates is an important factor in determining host response and risk of osteolysis.[58] Finally, only one implant size was investigated in this study, so it is currently unknown how different implant sizes would affect wear rates.

In conclusion, this study has demonstrated that a canine hip resurfacing implant with a 1.5 mm thick liner made of highly cross-linked polyethylene will not fracture or have excessive wear after 1.1. million cycles. This thin liner can enable the use of a large, more physiologic femoral head to support a return to an active lifestyle. The hip resurfacing device developed in this study may improve the standard of care for canines with hip osteoarthritis, and since canines are the preferred animal model for young, active THA patients,[22,23] this device can assist the evaluation and optimization of MoP hip resurfacing devices for human patients.

AUTHORS' CONTRIBUTIONS

Kevin J. Warburton: Designed, assembled, and validated the canine hip simulator used for wear testing. Designed the wear testing protocol. Wrote first draft of the manuscript. John B. Everingham: Developed and validated mechanoelectronic and heating aspects of our test system. Redesigned components of the hip simulator and assisted all experiments. Jillian L. Helms: Developed gravimetrics protocol. Led effort on all wear testing experiments. Andrew J. Kazanovicz: Lead engineer on the development of the canine hip resurfacing implant. Supervised efforts to design the metal backing and the thin polyethylene liner. Katherine A. Hollar: Developed, validated, and implemented a protocol using a structured-light 3D scanning system

to measure surface wear. Jeff D. Brourman: Primary clinical support. Provided clinical input on hip resurfacing design and wear testing protocol. Steven M. Fox: Clinical support and project management. Directed efforts to manufacture the hip resurfacing implant. Trevor J. Lujan: Supervised all elements of project. Wrote final draft of the manuscript. All authors have read and approved the final submitted manuscript.

ACKNOWLEDGMENTS

This material is based upon work supported by the Idaho Global Entrepreneurial Mission and the National Institute of General Medical Sciences of the National Institutes of Health under Award Number P20GM109095. A special thanks to Phil Boysen, David Anderson, Olivia Doane, Daniel Burl, and Mary Beth Schmidt.

REFERENCES

1. Murphy LB, Helmick CG, Schwartz TA, et al. 2010. One in four people may develop symptomatic hip osteoarthritis in his or her lifetime. Osteoarthritis and Cartilage 18: 1372–1379.
2. Johnston SA. 1997. Osteoarthritis. Joint anatomy, physiology, and pathobiology. Vet Clin North Am Small Anim Pract 27:699–723.
3. Rialland P, Bichot S, Moreau M, et al. 2012. Clinical validity of outcome pain measures in naturally occurring canine osteoarthritis. BMC Vet Res 8:1.
4. Puolakka TJ, Pajamäki KJJ, Halonen PJ, et al. 2001. The Finnish Arthroplasty Register: report of the hip register. Acta Orthop Scand 72:433–441.
5. Kishida Y, Sugano N, Nishii T, et al. 2004. Preservation of the bone mineral density of the femur after surface replacement of the hip. Bone Joint J 86:185–189.
6. Girard J, Miletic B, Deny A, et al. 2013. Can patients return to high-impact physical activities after hip resurfacing? A prospective study. Int Orthop 37:1019–1024.
7. Coulter G, Young D, Dalziel R, et al. 2012. Birmingham hip resurfacing at a mean of ten years. J Bone Joint Surg Br 94:315–321.
8. Le Duff MJ, Wang CT, Wisk LE, et al. 2010. Benefits of thin-shelled acetabular components for metal-on-metal hip resurfacing arthroplasty. J Orthop Res 28:1665–1670.
9. Girard J, Lavigne M, Vendittoli P-A, et al. 2006. Biomechanical reconstruction of the hip. Bone Joint J 88:721–726.
10. Aqil A, Drabu R, Bergmann JH, et al. 2013. The gait of patients with one resurfacing and one replacement hip: a single blinded controlled study. Int Orthop 37:795–801.
11. Williams DH, Greidanus NV, Masri BA, et al. 2011. Prevalence of pseudotumor in asymptomatic patients after metal-on-metal hip arthroplasty. J Bone Joint Surg Am 93: 2164–2171.
12. De Haan R, Pattyn C, Gill H, et al. 2008. Correlation between inclination of the acetabular component and metal ion levels in metal-on-metal hip resurfacing replacement. Bone Joint J 90:1291–1297.
13. Langton D, Jameson S, Joyce T, et al. 2008. The effect of component size and orientation on the concentrations of metal ions after resurfacing arthroplasty of the hip. Bone Joint J 90:1143–1151.
14. Rodriguez de la Flor M, Hernandez-Vaquero D, Fernandez-Carreira JM. 2013. Metal presence in hair after metal-on-metal resurfacing arthroplasty. J Orthop Res 31:2025–2031.
15. Kwon YM, Thomas P, Summer B, et al. 2010. Lymphocyte proliferation responses in patients with pseudotumors following metal-on-metal hip resurfacing arthroplasty. J Orthop Res 28:444–450.
16. Pritchett JW. 2016. Hip resurfacing using highly cross-linked polyethylene: prospective study results at 8.5 years. J Arthroplasty 31:2203–2208.
17. Illgen RL, Forsythe TM, Pike JW, et al. 2008. Highly crosslinked vs conventional polyethylene particles—an in vitro comparison of biologic activities. J Arthroplasty 23: 721–731.
18. Amstutz HC, Takamura KM, Ebramzadeh E, et al. 2015. Highly cross-linked polyethylene in hip resurfacing arthroplasty: long-term follow-up. Hip Int 25:39–43.
19. Buechel FF, Pappas MJ. 2011. A metal/ultrahigh-molecular-weight polyethylene cementless surface replacement. Semin Arthroplasty 22:66–74.
20. An YH, Friedman RJ. 1998. Animal models in orthopaedic research. Animal selections in orthopaedic research. Boca Raton, FL: CRC Press LLC. p 39–57.
21. Goethgen CB, Sumner DR, Platz C, et al. 1991. Changes in tibial bone mass after primary cementless and revision cementless total hip arthroplasty in canine models. J Orthop Res 9:820–827.
22. Skurla C, Pluhar G, Frankel D, et al. 2005. Assessing the dog as a model for human total hip replacement. Bone Joint J 87:120–127.
23. Skurla CP, James SP. 2005. Assessing the dog as a model for human total hip replacement: analysis of 38 postmortem-retrieved canine cemented acetabular components. J Biomed Mater Res B Appl Biomater 73:260–270.
24. Standardization IOf. 2014. ISO 11135: Sterilzation of healthcare –products – ethylene oxide – requirements for the development, validation and routine control of a sterilzation process for medical devices.78.
25. Standardization IOf. 2009. ISO 14242–3:2009, Implants for surgery – wear of total hip-joint prostheses – part 3: loading and displacement parameters for orbital bearing type wear testing machines and corresponding environnmental conditions for test.
26. Budsberg SC, Verstraete MC, Brown J, et al. 1995. Vertical loading rates in clinically normal dogs at a trot. Am J Vet Res 56:1275–1280.
27. Calonius O, Saikko V. 2002. Slide track analysis of eight contemporary hip simulator designs. J Biomech 35: 1439–1450.
28. Fu Y-C, Torres BT, Budsberg SC. 2010. Evaluation of a three-dimensional kinematic model for canine gait analysis. Am J Vet Res 71:1118–1122.
29. Lujan TJ, Lake SP, Plaizier TA, et al. 2005. Simultaneous measurement of three-dimensional joint kinematics and ligament strains with optical methods. J Biomech Eng 127: 193–197.
30. Saikko V, Calonius O. 2002. Slide track analysis of the relative motion between femoral head and acetabular cup in walking and in hip simulators. J Biomech 35:455–464.
31. Calonius O, Saikko V. 2003. Analysis of relative motion between femoral head and acetabular cup and advances in computation of the wear factor for the prosthetic hip joint. Acta Polytech 43:43–54.
32. ASTM. 1996. Gravimetric wear assessment of prosthetic hip-designs in simulator devices.
33. Standardization IOf. 2000. ISO 14242–2:2000, Implants for surgery – wear of total hip-joint prostheses – part 2: methods for measurement.
34. Wang A, Sun D, Stark C, et al. 1995. Wear mechanisms of UHMWPE in total joint replacements. Wear 181:241–249.

35. Rieker CB, Schön R, Konrad R, et al. 2005. Influence of the clearance on in-vitro tribology of large diameter metal-on-metal articulations pertaining to resurfacing hip implants. Orthop Clin N Am 36:135–142.
36. Spencer RF. 2011. Evolution in hip resurfacing design and contemporary experience with an uncemented device. J Bone Joint Surg Am 93:84–88.
37. Tan TL, Ebramzadeh E, Campbell PA, et al. 2014. Long-term outcome of a metal-on-polyethylene cementless hip resurfacing. J Arthroplasty 29:802–807.
38. Sayeed SA, Mont MA, Costa CR, et al. 2011. Early outcomes of sequentially cross-linked thin polyethylene liners with large diameter femoral heads in total hip arthroplasty. Bull NYU Hosp Joint Dis 69:S90.
39. Markel D, Day J, Siskey R, et al. 2011. Deformation of metal-backed acetabular components and the impact of liner thickness in a cadaveric model. Int Orthop 35:1131–1137.
40. Medley JB. 2016. Can physical joint simulators be used to anticipate clinical wear problems of new joint replacement implants prior to market release? Proc Inst Mech Eng 230: 347–358.
41. Affatato S, Zavalloni M, Taddei P, et al. 2008. Comparative study on the wear behaviour of different conventional and cross-linked polyethylenes for total hip replacement. Tribol Int 41:813–822.
42. Moro T, Takatori Y, Kyomoto M, et al. 2015. Wear resistance of the biocompatible phospholipid polymer-grafted highly cross-linked polyethylene liner against larger femoral head. J Orthop Res 33:1103–1110.
43. Loving L, Herrera L, Banerjee S, et al. 2015. Dual mobility bearings withstand loading from steeper cup-inclinations without substantial wear. J Orthop Res 33:398–404.
44. Trommer RM, Maru MM. 2017. Importance of preclinical evaluation of wear in hip implant designs using simulator machines. Rev Bras Ortop 52:251–259.
45. Affatato S, De Mattia JS, Bracco P, et al. 2016. Wear performance of neat and vitamin E blended highly cross-linked PE under severe conditions: the combined effect of accelerated ageing and third body particles during wear test. J Mech Behav Biomed Mater 64:240–252.
46. Spinelli M, Affatato S, Tiberi L, et al. 2010. Integrated friction measurements in hip wear simulations: short-term results. Proc Inst Mech Eng H 224:865–876.
47. Atwood SA, Van Citters DW, Patten EW, et al. 2011. Tradeoffs amongst fatigue, wear, and oxidation resistance of cross-linked ultra-high molecular weight polyethylene. J Mech Behav Biomed Mater 4:1033–1045.
48. Johnson AJ, Loving L, Herrera L, et al. 2014. Short-term wear evaluation of thin acetabular liners on 36-mm femoral heads. Clin Orthop Relat Res 472:624–629.
49. Affatato S, Bersaglia G, Rocchi M, et al. 2005. Wear behaviour of cross-linked polyethylene assessed in vitro under severe conditions. Biomaterials 26:3259–3267.
50. McKellop H, Shen F-w, DiMaio W, et al. 1999. Wear of gamma-crosslinked polyethylene acetabular cups against roughened femoral balls. Clin Orthop Relat Res 369:73–82.
51. Oral E, Christensen SD, Malhi AS, et al. 2006. Wear resistance and mechanical properties of highly cross-linked, ultrahigh-molecular weight polyethylene doped with vitamin E. J Arthroplasty 21:580–591.
52. Saikko V, Calonius O, Keränen J. 2002. Wear of conventional and cross-linked ultra-high-molecular-weight polyethylene acetabular cups against polished and roughened CoCr femoral heads in a biaxial hip simulator. J Biomed Mater Res 63:848–853.
53. Taddei P, Tozzi S, Carmignato S, et al. 2016. May the surface roughness of the retrieved femoral head influence the wear behavior of the polyethylene liner? J Biomed Mater Res B Appl Biomater 104:1374–1385.
54. Chan CB, Spierenburg M, Ihle SL, et al. 2005. Use of pedometers to measure physical activity in dogs. J Am Vet Med Assoc 226:2010–2015.
55. Sychterz CJ, Engh CA, Jr., Yang, et al. 1999. Analysis of temporal wear patterns of porous-coated acetabular components: distinguishing between true wear and so-called bedding-in. J Bone Joint Surg Am 81:821–830.
56. Wroblewski BM, Siney PD, Dowson D, et al. 1996. Prospective clinical and joint simulator studies of a new total hip arthroplasty using alumina ceramic heads and cross-linked polyethylene cups. J Bone Joint Surg Br 78: 280–285.
57. Kelly NH, Rajadhyaksha AD, Wright TM, et al. 2010. High stress conditions do not increase wear of thin highly cross-linked UHMWPE. Clin Orthop Relat Res 468:418–423.
58. de Villiers D, Shelton JC. 2016. Measurement outcomes from hip simulators. Proc Inst Mech Eng H 230:398–405.